INTERNATIONAL JOURNAL FOR NUMERICAL METHODS IN FLUIDS
Int. J. Numer. Meth. Fluids 2009; **59**:817–826
Published online 19 August 2008 in Wiley InterScience (www.interscience.wiley.com). DOI: 10.1002/fld.1832

SHORT COMMUNICATION

Numerical investigation of hemodynamics at an end-to-side junction with a laterally diffused bypass graft

Yong Hyun Kim and Joon Sang Lee*, †

Department of Mechanical Engineering, Wayne State University, Detroit, MI, U.S.A.

SUMMARY

Intimal hyperplasia (IH) at arterial bypass graft is a major factor responsible for graft failure. Several techniques are used to explain IH formation at the end-to-side anastomosis junction. Abnormal hemodynamics contributing to the development of disease at the junction is the one of most common theories. This study describes a means of modifying the area of bypass graft at the junction part. This procedure, called the laterally diffused bypass graft (LDBG), is able to alter the hemodynamics in the end-to-side anastomosis. The LDBG model, due to an expansion of the outer curvature in the graft, reduces the velocity on the artery bed, side and top junction walls. The recirculation with velocity vectors on the host artery is significantly altered near the heel region on the host artery. Wall shear stress is decreased by up to 34% on the floor of artery centerline at the peak systole and by 61.9% on the top junction of artery during the systole deceleration. Corresponding time-averaged wall shear stresses are found to decrease by 40.5%. Secondary flow is observed to be decreased significantly at the distal junction. Copyright © 2008 John Wiley & Sons, Ltd.

Received 22 January 2008; Revised 25 March 2008; Accepted 30 March 2008

KEY WORDS: hemodynamics; laterally diffused bypass graft; anastomosis

INTRODUCTION

Vascular disease with narrowing peripheral arteries is one of the common manifestations of atherosclerosis. Bypass grafting, using an autologus vein or prosthetic graft, is commonly employed to restore a circulation to the lower extremities [1, 2]. Anastomotic intimal hyperplasia (IH) causes the gradual narrowing of the vessel lumen and is one of the principal causes of failure of bypass

*Correspondence to: Joon Sang Lee, Department of Mechanical Engineering, Wayne State University, 5050 Anthony Wayne Dr. #2100, Detroit, MI 48202, U.S.A.
†E-mail: joonlee@wayne.edu

grafts [3, 4]. This abnormal, progressive thickening of the artery wall is observed to occur predominantly at the distal anastomosis of a bypass, being especially prominent at the heel, toe and along the suture line where the graft is fixed to the recipient vessel, and on the artery floor [5].

Although many theories of IH have been postulated, the exact mechanism of IH remains uncertain, with indications that mechanical factors are involved [6–9]. With respect to biological effects, endothelial cell and smooth muscle cell proliferations are major contributors to IH and that a platelet-derived growth factor may be responsible [7]. Mechanical factors interact with the biological factors and include vascular wall stresses and luminal hemodynamics [8, 9]. The fluid dynamics within vascular grafts is also believed to be highly related to the initiation and development of IH [10].

The Miller cuff, Taylor patch and Linton patch contain features that help to decelerate the flow into the host artery, thereby reducing the peak wall shear stress (WSS) magnitude acting along the host artery. It was hypothesized that the peak WSS acting on the artery wall were responsible for the increased incidence of IH development on the artery wall [4]. In this study, a laterally diffused area was modeled in the design process of the bypass graft to decelerate the flow into the host artery, in an attempt to reduce peak WSS magnitude acting along the top and floor.

NUMERICAL METHODS

There were two different numerical models to be compared for comparative purposes. They are namely a conventional and modified end-to-side anastomosis with laterally diffused area. The cylindrical tube intersecting 45° represented an idealized geometry of an end-to-side bypass anastomosis [11]. The diameters of host artery and bypass graft artery were 7 mm ($D=2R$, R is a radius of host artery) at an angle of 45° in Figure 1(a). The modified graft outlet area, laterally diffused bypass graft (LDBG), had the same diameter of the conventional bypass graft (CBG), but it had a diffused area on the outside of graft curvature near an anastomosis. The length of the modified part was $2R$. The CBG and LDBG models were meshed with 9124 and 10 034 quadrilateral elements. The comparison of CBG and LDBG models is shown in Figure 1(b).

Blood flow had the attributes of three-dimensional, time-dependent, incompressible, isothermal and laminar flow. The governing equations for such a flow were

$$\nabla \cdot u = 0 \tag{1}$$

$$\rho \frac{\partial u}{\partial t} + \rho(u \cdot \nabla)u = -\nabla p + \nabla \cdot (\mu \nabla u) \tag{2}$$

where u is the velocity vector, ρ is the density, t is the time and p is the pressure.

The meshes were created by Gambit 2.1 (Fluent Inc.) and processed using the finite volume solver Fluent 6.2 (Fluent Inc.). Models were solved on Dell Precision 470, Xeon 3 GHz workstation with 2 GB RAM. Grid independence for the velocity profile through several cross sections was specified as having the results of interest within 3% of their limiting values. The resulting system of algebraic equations was solved iteratively using a procedure based on the semi-implicit SIMPLE algorithm. Time stepping employed a fully implicit scheme. The end-to-side anastomosis CFD model has been validated by comparing calculated results with the measured data for velocity and

DOI: 10.1002/fld

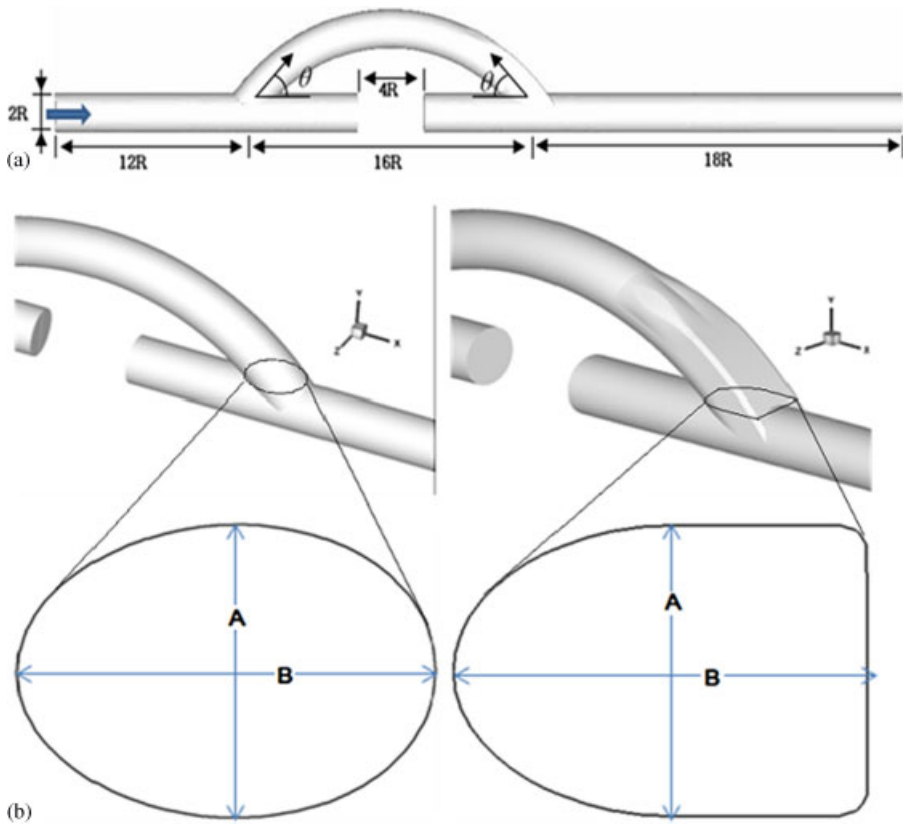

Figure 1. (a) Geometry of a bypass graft. (b) Schematic drawing of a distal vascular anastomosis. Bypass grafts have the same diameter, $2R$, as the host artery. The cross-sectional area of a junction anastomosis is elliptic in the CBG model, but the extended area in the LDBG model.

concentration obtained from experimental technique [12]. The conventional model in the Fluent code was successfully applied by reanalyzing flow characteristics for the application of blood flow in an end-to-side anastomosis [13].

A parabolic pulsatile inlet velocity profile was applied at the inlet of the geometry as shown in Figure 2. The maximum Reynolds number during the cycle was about 540, which is a characteristic of patient in a resting condition [14]. The outlet reference pressure was set to $1.02 \times 10^4\,\mathrm{kg/ms}$ (75 mmHg) above atmospheric, which is an average aortic pressure from *in vivo* measurement [15]. Results were presented at times during the cycle representative of systole acceleration V_a, peak systole V_p and systole deceleration V_d. These points have been found to be important in a previous study [5]. The computation of three cycles was necessary in order to eradicate any start-up effects and achieve repeatability between flow patterns computed in successive cycles.

Rigid walls were assumed and the no-slip condition was enforced on all walls. The convergence criterion was set to 0.001 for the residuals of the continuity equation and of X, Y and Z momentum equations. The blood was modeled as a Newtonian fluid with a viscosity of 0.0035 Pa s. Blood density was 1080 kg/m [3].

DOI: 10.1002/fld

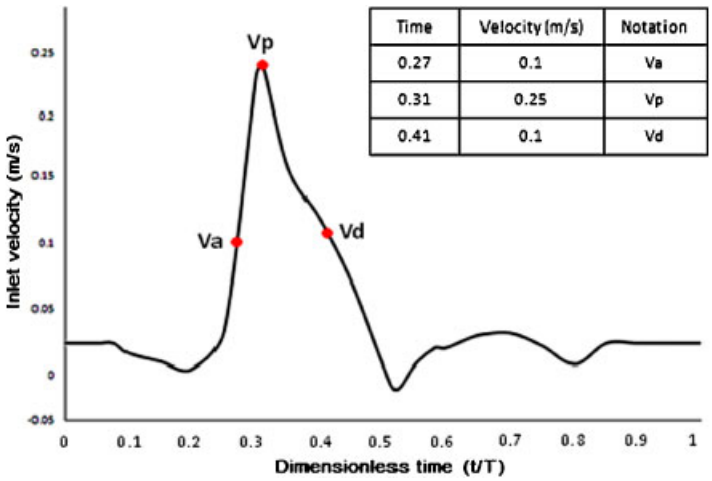

Time	Velocity (m/s)	Notation
0.27	0.1	Va
0.31	0.25	Vp
0.41	0.1	Vd

Figure 2. Velocity pulsatile of the blood in the resting state. The pulse points of interest for results acquisition are shown in the table.

RESULTS

In general, the flow behaviors at the proximal and distal anastomosis displayed considerable spatial and temporal variations. This paper concentrated on the flow at distal junction, since the disease development was more critical in that region.

It is evident that the effect of the LDBG procedure is significant enough to gradually reduce the average velocity of the blood as it approaches the distal anastomosis. This is due to that fact that the cross-sectional area of the bypass is steadily becoming larger. This enlargement of the cross-sectional area prevents the sudden deceleration experienced by the fluid returning to the host vessel in the CBG model.

The influences of the LDBG design are pronounced at V_p and V_d, while local flow characteristics are low at V_a as shown in Figure 3. In those cases, the decrease in the momentum possessed by fluid arriving at the distal anastomosis ensures that the blood is guided more smoothly through the junction.

By skewing of the flow within the bypass graft, as the fluid turns through the anastomosis, secondary flows are generated. Figure 4 traces and contrasts the development of the secondary flow at one arterial diameter distal to the toe in the two cases. The strong secondary flow and maximum velocity magnitude appeared in the CBG model decrease when the LDBG model is applied. During all time steps, secondary flow in the LDBG model is almost negligible, yet it is already developing in the CBG model. In comparison, it is clear that the cross-flow continues to play a more instrumental role in the CBG model.

The effect of the altered hemodynamics on the floor of the artery may be qualified further by examining WSS contour plots as shown in Figure 5. Large WSS magnitudes are found during the systole as the powerful systolic flow impacts the floor of the artery. Significant differences are evident at V_p and V_d, whereas the differences are small at V_a. The WSS magnitude on the artery floor always seems to be small with the LDBG model, while the CBG model has high WSS magnitudes. The diminution of the anastomotic flow disturbances with increasing distance distally is observed.

DOI: 10.1002/fld

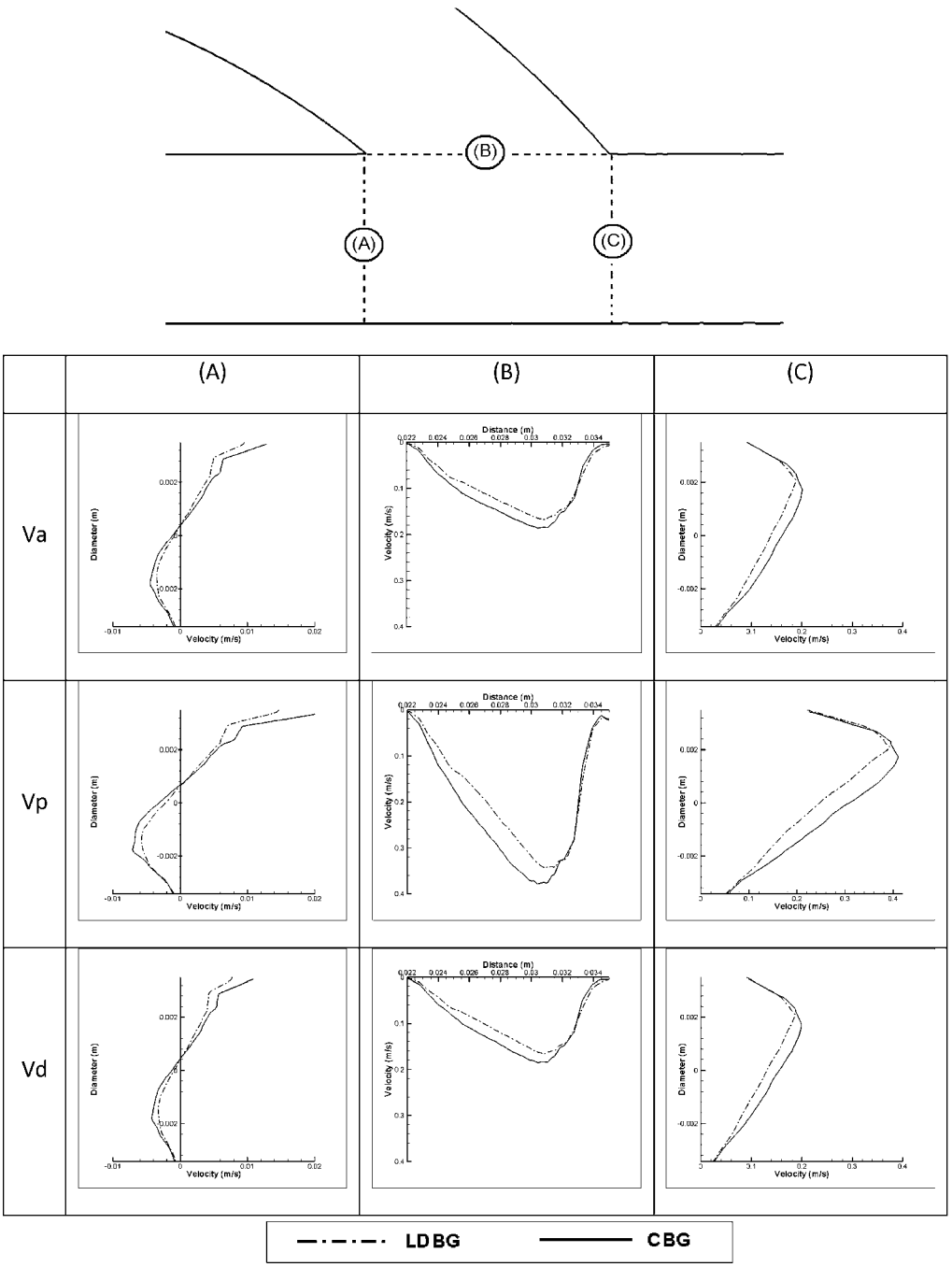

Figure 3. The center-plane vector plots at V_a (a), V_p (b) and V_d (c) for the CBG (left) and the LDBG (right). The development of a flow recirculation region and flow separation region is clearly evident in the conventional anastomosis but not so in the modified anastomosis.

DOI: 10.1002/fld

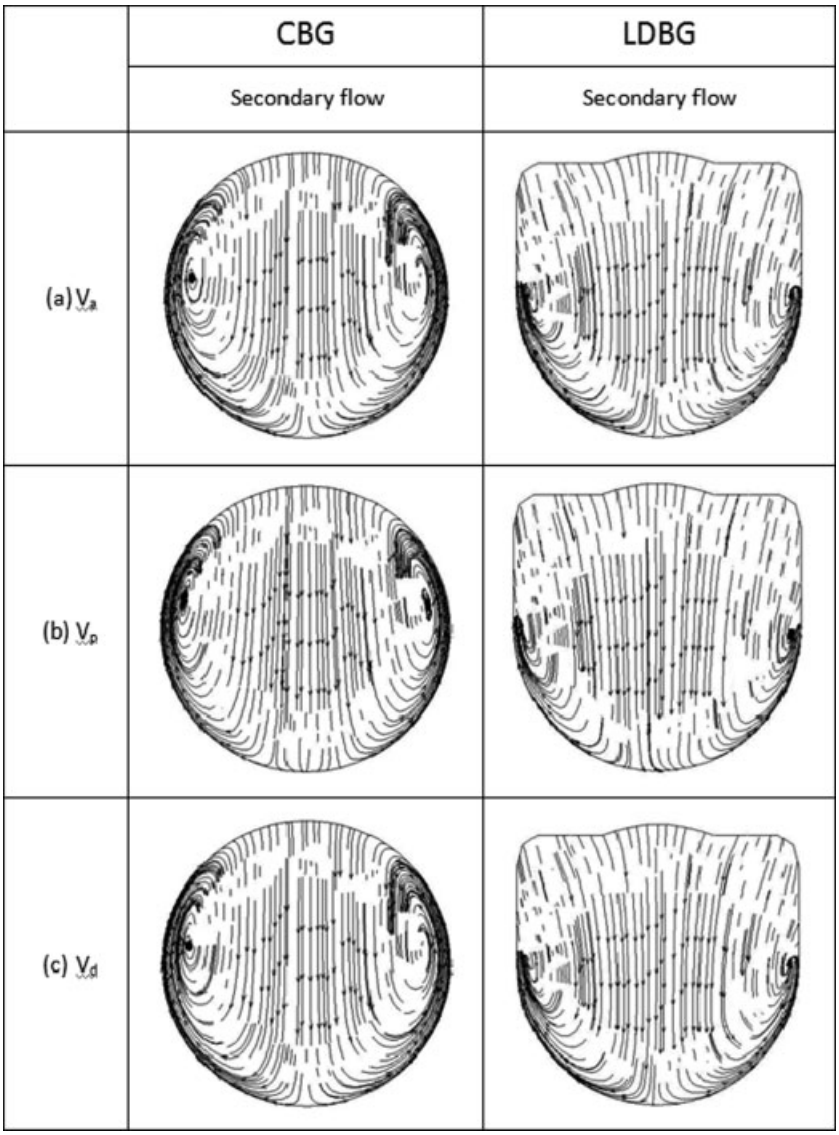

Figure 4. Velocity magnitude and secondary flow profiles in the host artery at V_a, V_p and V_d. The cross section is taken through the toe and parallel to the $Y-Z$ plane. The maximum velocity magnitude and the size of secondary flow regions decrease due to the LDBG.

It is clear that the addition of the LDBG graft affects the WSS distribution along the top and floor of the artery during the systole in Figure 6. Along the top of the artery (Figure 6(a)), the peak WSS significantly decreases near the toe region in the LDBG model (by 65.3% at V_d). In addition, along the floor of the artery (Figure 6(b)), the peak WSS is less extreme in the LDBG model (decreased by 5.3% at V_d). The large negative shear stress is also weaker in the LDBG

DOI: 10.1002/fld

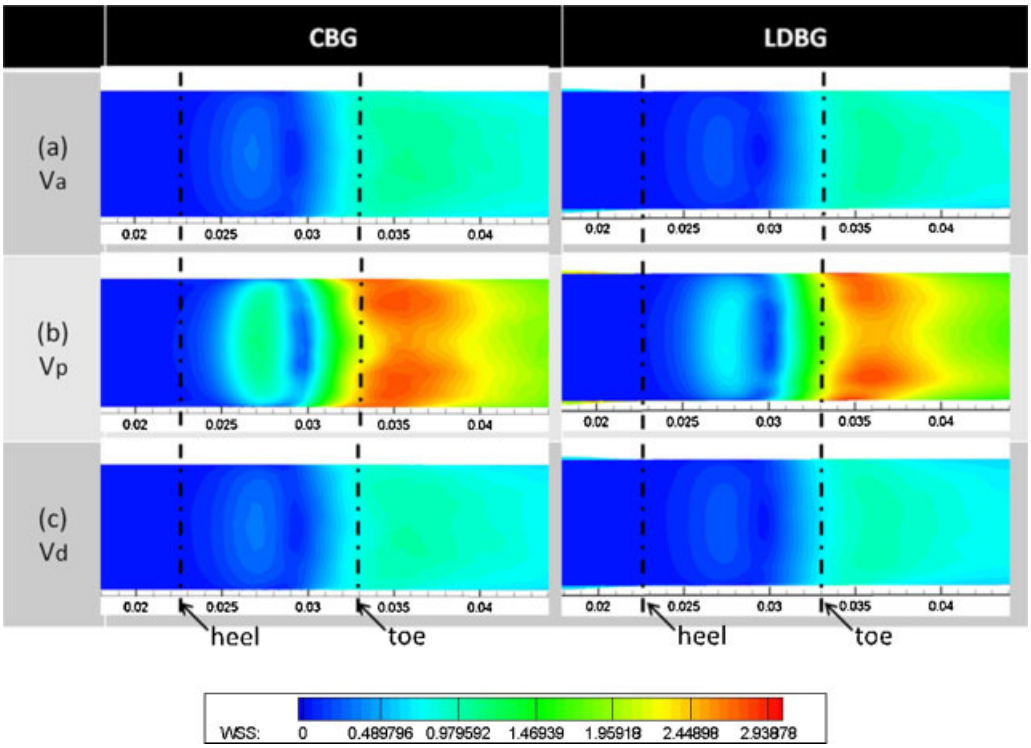

Figure 5. The WSS of CBG (left) is compared with LDBG (right) for the floor of the artery. The LDBG reduces the pressure difference thereby reducing WSS.

model, which is associated with the recirculation (decreased by 33.99% at V_p). In Figure 6(c), the corresponding time-averaged wall shear stresses (TAWSS) magnitude decreases by 40.5% near the heal region in the LDBG model.

The adjusted geometry of the LDBG model causes the momentum of the blood to be reduced on approach to the distal anastomosis. Therefore, in that case, as the blood flows into the recipient artery, flow across the channel is not as prevalent as in the CBG model. The enlarged area in the LDBG model ensures that the heel recirculation is less constricted against the artery floor, accounting for the decreased WSS magnitudes observed in that locality during systole.

DISCUSSION AND CONCLUSION

The abnormality of the conventional junction model has been studied and reduced with developing bypass graft models. IH mainly occurs on the suture line and artery floor and causes the graft failure. Numerous studies have been performed to find the disease-influencing factors in the end-to-side anastomosis [11]. It is clear that abnormality of hemodynamics leads to arterial responses that promote disease [16]. *In vitro* and numerical studies have confirmed that the anastomotic flow patterns are strongly dependent on the local geometry [17].

DOI: 10.1002/fld

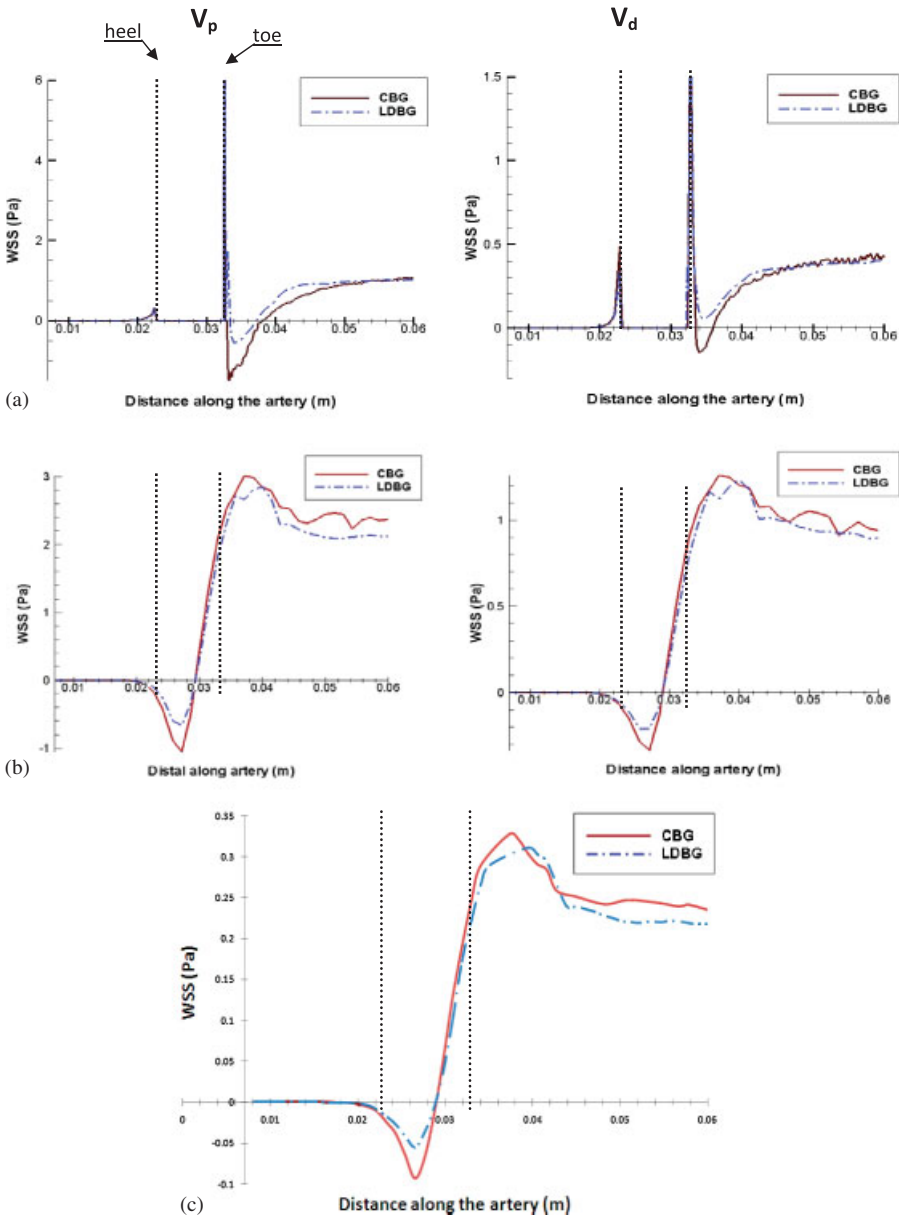

Figure 6. WSS at the junction (toe and heel) (a) and at the floor (b) of artery and TAWSS at the floor of the artery (c) at V_p and V_d for the two models. There are significant reductions in WSS and TAWSS of the floor and top of artery when the LDBG model is applied.

DOI: 10.1002/fld

The Miller cuff and Taylor patch aimed to buffer the material mismatch between the compliant artery and the stiff graft and sought to decelerate the flow through the junction. It needed a new method to increase the lifetime of the anastomosis junction while limited studies of these surgical techniques might provide an adequate success.

This study used an LDBG to attempt to reduce abnormality of hemodynamics from the more disease prone artery bed. It was clear that the extended area of the junction affects the hemodynamics through the anastomosis. Fluid separation arose just distal to the toe during the peak systole and systole deceleration, in the CBG model. The progression of IH at the toe region should be alleviated in the LDBG model in which flow separation was reduced and where the graft surface has been extended. In addition, secondary flow profiles were altered and diminished at the toe region with the LDBG model.

There were a number of limitations with this study. The principal changes only have been reported in the entire flow field. While certain studies suggested that WSS and TAWSS on the artery floor may have played a role in disease formation, and that control of these variables was worthy of investigation, numerous other studies existed citing a range of factors not quantified here as also playing a role. In addition, the effects of material mismatch have been neglected.

The results of this numerical study have shown that the modification of the anastomosis geometry associated with the LDBG model clearly influenced the local flow behavior. Recirculation size, WSS and TAWSS magnitudes decreased along the floor and junction of artery, especially near the heel region on the artery floor and near the toe region on the junction of artery. Therefore, it could be considered how the modified hemodynamic environment may contribute to the enhanced success rates of the LDBG model.

REFERENCES

1. Archie JP. Femoropopliteal bypass with either adequate ipsilateral reversed saphenous vein or obligatory polytetraflorethylene. *Annals of Vascular Surgery* 1994; **8**(5):475–484.
2. Taylor RS, Loh A, McFarland RJ, Cox M, Chester JF. Improved techniques for PTFE bypass grafting: long-term results using anastomotic vein patches. *British Journal of Surgery* 1992; **79**:348–354.
3. Chervu A, Moore W. An overview of intimal hyperplasia. *Surgery Gynecology and Obstetrics* 1990; **171**:433–447.
4. Walsh M, Kavanagh E, O'Brien T, Grace P, McGloughlin T. On the existence of an optimum end-to-side junctional geometry in peripheral bypass surgery—a computer generated study. *European Journal of Vascular and Endovascular Surgery* 2003; **26**:649–656.
5. Sottiurai VS, Yao JS, Batson RC, Sue SL, Jones R, Nakamura YA. Distal anastomotic intimal hyperplasia: histopathologic character and biogenesis. *Annals of Vascular Surgery* 1989; **3**:26–33.
6. Bandyk DF, Seabrook GR, Moldenhauer P. Hemodynamics of vein graft stenosis. *Journal of Vascular Surgery* 1988; **8**:688–695.
7. Clowes AW, Kirkman TR, Clowes MM. Mechanism of arterial graft failure. II. Chronic endothelial and smooth muscle cell proliferation in healing PTFE prosthese. *Journal of Vascular Surgery* 1986; **3**:877–884.
8. Hyun S, Kleinstreuer C, Archie Jr JP. Hemodynamics analyses of arterial expansions with implications to thrombosis and restenosis. *Medical Engineering and Physics* 2000; **22**:13–27.
9. Kraiss LW, Geary RL, Mattsson EJR, Vergel S, Au YPT, Clowes AW. Acute reductions in blood flow and shear stress induce platelet-derived growth factor—a expression in baboon prosthetic grafts. *Circulation Research* 1996; **79**:45–53.
10. Madras PN, Ward CA, Johnson WR, Singh PI. Anastomotic hyperplasia. *Surgery* 1981; **90**:922–923.
11. Hofer M, Rappitsch G, Perktold K, Trubel W, Schima H. Numerical study of wall mechanics and fluid dynamics in end-to-side anastomoses and correlation to intimal hyperplasia. *Journal of Biomechanics* 1996; **29**(10):1297–1308.
12. Lei M, Giddens DP, Jones SA, Loth F, Bassiouny H. Pulsatile flow in an end-to-side vascular graft model: comparison of computations with experimental data. *Journal of Biomechanical Engineering* 2001; **123**: 80–87.

DOI: 10.1002/fld

13. Cole JS, Watterson JK, O'Reilly MJG. Numerical investigation of the hemodynamics at a patched arterial bypass anastomosis. *Medical Engineering and Physics* 2002; **24**:393–401.
14. Milnor W. *Hemodynamics* (2nd edn). Williams and Wilkins: Baltimore, 1989.
15. Poppas A, Shroff SG, Korcarz CE, Hibbard JU, Berger DS, Lindheimer MD, Lang RM. Serial assessment of the cardiovascular system in normal pregnancy—role of arterial compliance and pulsatile arterial load. *Circulation* 1997; **95**:2407–2415.
16. Resnick N, Gimbrone MA. Hemodynamic forces are complex regulators of endothelial gene expression. *FASEB Journal* 1995; **9**:874–882.
17. Lei M, Kleinstreuer C, Archie JP. Geometric design improvements for femoral graft-artery junctions mitigating restenosis. *Journal of Biomechanics* 1996; **29**:1605–1614.

DOI: 10.1002/fld